Nanoplankton dominate autumn biomass on the Agulhas Bank

Sixolile L. Mazwane[1], Alex J. Poulton[2], Margaux Noyon[1], Emma Rocke[3], Mike J. Roberts[1,4]

[1]Department of Oceanography and Institute for Coastal and Marine Research, Nelson Mandela University, Port Elizabeth 6001, South Africa.

[2]The Lyell Centre for Earth and Marine Science, Heriot-Watt University, Riccarton Campus, Edinburgh, EH14 4AP, UK.

[3]Department of Biological Sciences and Marine Research Institute, University of Cape Town, Cape Town 7701, South Africa

[4]School of Ocean and Earth Sciences, University of Southampton, Southampton, United Kingdom

Corresponding author: Sixolile Mazwane (Smazwane46@gmail.com)

ORCID IDs

Sixolile Mazwane (0000-0001-8707-3111)

Alex Poulton (0000-0002-5149-6961)

Margaux Noyon (0000-0002-0761-4174)

Emma Rocke (0000-0001-9514-9788)

Mike Roberts (0000-0003-3231-180X)

Key points:

- Nanoplankton dominate carbon (>80% total) biomass in autumn on the Agulhas Bank.
- Nanoplankton dominance highlights micro-zooplankton grazing for trophic transfer.
- Nanoplankton and micro-zooplankton key to productive Agulhas Bank ecosystems.

Abstract

Autumn productivity is key to the large marine ecosystems of the Agulhas Bank, which support numerous economically important regional fisheries. Despite such importance, data is sparce on plankton composition in terms of primary or secondary producers, or on trophic transfer. While investigating autumn plankton composition we found that nanophytoplankton (2-20 µm) dominated carbon stocks, with lower contributions from picophytoplankton (<2 µm) and microphytoplankton (>20 µm). While picoplankton biomass exhibited a relationship with warm nutrient poor waters, nanoplankton showed no clear relationship to environmental parameters. The dominance of nanophytoplankton biomass on the Agulhas Bank highlights a critical role for micro-zooplankton grazing as a trophic transfer between these small plankton, meso-zooplankton and the higher trophic levels that make the bank so important for regional fisheries. Outside of localized coastal upwelling on the Agulhas Bank, this study highlights a significant role for nanoplankton and micro-zooplankton in supporting the bank's large marine ecosystems.

Plain Language Summary

Phytoplankton support productive marine ecosystems through provision of primary production and biomass, with their size-structure determining the efficiency of transfer of energy through the ecosystem. Dominance of small phytoplankton (<20 µm) leads to longer food chains and transfer of energy and biomass to higher trophic levels. Observations of the Agulhas Bank plankton community in autumn, a period of important primary productivity for the region, found a dominance of small nanoplankton (2-20 µm) in terms of biomass. Nanoplankton dominance has important implications for how the Agulhas Bank ecosystem function, highlighting a significant role for micro-zooplankton. The Agulhas Bank is a data sparce environment currently no research on micro-zooplankton has focused on the Agulhas Bank and this is an obvious important group to study further to better understand how the marine ecosystem supports the key regional fisheries that rely on this area.

1. Introduction

Phytoplankton support marine food webs and the carbon cycle, accounting for ~50% of global net primary production (Field et al., 1998). Plankton size structure constrains ecosystem productivity (Marañón, 2015), determining the proportion of production passed to higher trophic levels, recycled or exported to the deep sea (Acevedo-Trejos et al., 2015). Phytoplankton may be split into different size categories (Sieburth, 1979): picoplankton (cell diameters 0.2-2 µm), nanoplankton (2-20 µm) and microplankton (>20 µm). The small cell diameters of pico- and nano-plankton are not grazed by meso-zooplankton (>200 µm) (Huggett et al., 2023, Mitra et al., 2023), and instead are predated by micro-zooplankton (20-200 µm) who then may be grazed by larger zooplankton.

Picoplankton are made up of the cyanobacteria *Prochlorococcus* (PRO) and *Synechococcus* (SYN) (Waterbury et al., 1979; Chisholm et al., 1988; Rajaneesh et al., 2017), and a diverse set of pico-eukaryotes (PICO) (Worden, 2006). SYN and PICO favor light and nutrient rich waters (Moore et al., 2003; Rajaneesh et al., 2015). Nanoplankton (NANO, 2-20 µm) include a diverse number of taxa, including Haptophytes, Pelagophytes, and Cryptophytes (CRYPTO) (Flander-Putrle et al., 2021), with haptophytes often dominating (Liu et al., 2009). Larger microplankton (>20 µm) are most frequently associated with diatoms and dinoflagellates (Rajaneesh et al., 2017; Lamont et al., 2018).

PRO and SYN have overlapping ecological niches of warm low-nutrient waters and may contribute up to 80% of phytoplankton biomass and productivity (Scanlan et al., 2009; Wang et al., 2022), despite their relatively small size (0.5-0.7 µm and 0.7-1.2 µm, respectively) and cell carbon content (Tarran et al., 2006). PICO are typically less abundant than PRO or SYN by at least an order of magnitude (Flombaum et al., 2020), though they contribute more to biomass due to their larger cell size (0.2-3 µm) and carbon content (Moran, 2015).

Shelf seas make a disproportional contribution to primary production compared to their areal extent (Field et al., 1998), supporting ~ 90% of economically important fisheries (Pauly et al., 2002). Shelf seas are often regarded as microplankton dominated, though little is known of the smaller plankton in these systems (van Dongen-Vogels et al., 2011, 2012; Daneri et al., 2012).

The Agulhas Bank (AB) is a moderately productive shelf (Mazwane et al., 2022) that supports complex trophic structures and numerous commercially harvested marine resources (Hutchings et al., 2009; Lamont et al., 2018). Analysis of satellite and pigment data from the AB has highlighted microplankton dominance in inner shelf waters, with nanoplankton in the adjacent ocean (Barlow et al., 2010; Lamont et al., 2018; Sonnekus, 2022), though such studies have focused on the eastern AB rather than the wider bank.

To explore the gap in knowledge of the AB plankton in terms of pico- and nano-plankton, we undertook flow cytometry (Marie et al., 1997; van Dongen-Vogels et al., 2011) of the small phytoplankton (<20 µm) during an autumn (2019) cruise (Figure 1a). Our objectives were to determine the (1) pico- and nano-plankton composition and distribution, (2) contribution of these groupings to carbon biomass, and (3) explore whether variability in composition and biomass were related to prevailing hydrographic gradients.

2. Material and Methods

2.1. Sampling

Sampling occurred on the AB onboard the *RV Ellen Khuzwayo* (cruise EK188, Noyon (2019), 21 March to 2 April 2019; n = 28) (Figure 1a). A Seabird 911+ V2 CTD system with rosette sampler was deployed, with water samples collected using 8 L Niskin bottles (OTE: Ocean Test Equipment), and sampling depths determined from temperature and fluorescence (WET Labs) profiles. Processing and calibration of CTD data followed standard procedures (see Noyon, 2019).

A CTD-mounted quantum PAR sensor (LiCor Inc., USA) determined the underwater light field and vertical attenuation coefficient of PAR (K_d, m^{-1}), with the depth of the euphotic zone as the depth that 1% surface irradiance penetrates (Poulton et al. 2022). Sea-surface Temperature (SST) was measured *in-situ* using a CTD-mounted temperature sensor. The surface mixed layer (SML) was determined as the depth of the maximum buoyancy frequency (Carvalho et al., 2017), with the maximum (N^2 max.) value used as a stratification index (Poulton et al., 2022). Average SML irradiance ($\bar{E}_{SML}$) was determined using a combination of K_d and SML (Poulton et al., 2011).

2.2. Flow Cytometry

Flow cytometry samples were collected from 4-5 depths, including sub-surface waters (~3 m), the beginning, maximum and lower limit of the fluorescence maximum, and below the strongest temperature gradient (thermocline). Seawater samples were pre-filtered through 200 μm mesh to remove zooplankton, and 2 mL triplicate aliquots were fixed in 0.25% glutaraldehyde (v/v, final concentration), flash frozen and stored (-80oC) prior to analysis.

Cell abundances (after Marie et al., 1997; van Dongen-Vogels et al., 2011) were determined on a LSRII (Becton Dickinson) flow cytometer with a 488-nm excitation laser and standard filter set (Campbell, 2001). FlowJo® software calculated PRO and SYN cell abundances. PICO, NANO and CRYPTO were measured through their respective signals emitted in orange (PE: 585/42 band pass) versus red (PC: 661/16 band pass) wavelengths. SYN abundance was distinguished from PICO and PRO through higher (per cell) phycoerythrin signals. The samples were thawed at room temperature and transferred to glass tubes and analyzed. Data were acquired at a medium flow rate with a threshold of ~10,000 events per run and the LSRII was calibrated daily using 3.0 μm Rainbow beads (Spherotech).

Cell abundances (cells mL^{-1}) were calculated from the mean of the triplicate samples, with relative standard deviations between triplicates ranging from 1-54% (average: 20%). Cell abundances were converted to cell biomass using literature values (Børsheim and Bratbak, 1987; Tarran et al., 2006): 2.7 fmol C $cell^{-1}$, Prochlorococcus (PRO); 8.58 fmol C $cell^{-1}$, Synechococcus (SYN); 36.67 fmol C $cell^{-1}$ for pico-eukaryotes (PICO); 0.26 pmol C $cell^{-1}$ for nanoeukaryotes (NANO); 0.26 pmol C $cell^{-1}$, for cryptophytes (CRYPTO).

For this study, the biomass integrations were calculated for the euphotic depth and MLD (see Table S1). The conversion values were chosen as values previously used for shelf waters rather than the open ocean. For NANO and CRYPTO, we used values from Børsheim and Bratbak (1987). Using Tarran et al. (2006) values would increase the NANO and CRYPTO biomass by 6.8% without changing the biomass patterns.

2.3. Size-fractionated Chlorophyll-*a* and Nutrients

Size-fractionated chlorophyll-a (Chl) concentrations (mg m^{-3}) were measured on 0.2 L water samples sequentially filtered through 20 µm, 2 µm and 0.2 µm 47-mm NucleoporeTM filters and extracted in 6 mL 90% acetone (Sigma-Aldrich, UK) at 4oC for 18-24 hr (Poulton et al., 2022). Chl fluorescence was measured on a Turner Designs TrilogyTM fluorometer using a non- acidification unit calibrated with solid and pure Chl standards (Sigma-Aldrich, UK).

Water samples for macronutrient concentrations were collected into acid-cleaned 50 mL HDPE bottles, which were frozen (-20°C) onboard and kept frozen until analysis (see Poulton et al., 2022). Concentrations (µmol L-1) of nitrate + nitrite (NO_3), phosphate (PO_4) and silicic acid ($Si(OH)_4$) were measured with a SEAL QuAAtro39 auto-analyzer following standard protocols (Becker et al., 2020). Certified reference materials were used daily (KANSO, Japan) and analytical procedures followed International GO-SHIP recommendations (Becker et al., 2020). The typical uncertainty of the analytical results were between 0.5% and 1%, and the limits for detection for NO_3 and PO_4 were 0.02 µmol L^{-1}, while Si(OH)4 was always higher than the detection limit (0.05 µmol Si L^{-1}). Deficiencies of NO_3 relative to PO_4 and $Si(OH)_4$ were described relative to the Redfield (1958) ratio, with N* (= NO_3 – (16 x PO_4); Moore et al., 2009), and relative to the 1:1 ratio of $Si(OH)_4$ to NO_3 uptake in diatoms (Brzezinski, 1985) through Si* (= $Si(OH)_4$ – NO_3; Bibby and Moore, 2011).

3. Results

3.1. Agulhas Bank Hydrography

A comprehensive overview of the hydrography of the AB during autumn (2019) is provided by Poulton et al. (2022), with the data included in Supplementary Table S1. SST ranged from 17-22°C (average (± standard deviation): 20 (± 1) °C) across the AB, with offshore stations generally showing higher SST (Table S2). SML in autumn showed an east (<10 m) to west (>20 m) deepening (Table S2), with the deepest SML at 27 m (average: 15 (± 5) m). SML deepening was related to warming of the SML, linked to the westward SST increase (Poulton et al., 2022). No clear or consistent inshore-offshore trends in the SML depth or SST were observed.

Euphotic zone depths ranged from 23-53 m (Table S2), with an average of 33 m (± 7 m) and no clear east to west or inshore-offshore trend was observed. ESML indicated that phytoplankton in the SML received irradiances ranging from 26-63% (average: 44 (± 10) %)

of the incidental irradiance (Table S2). An east to west trend was observed, with the irradiance decreasing towards the west as the SML deepened (Table S1, Poulton et al., 2022).

The maximum value of the buoyancy frequency (N^2 max.), an indicator of water column stratification, showed an east to west strengthening (Table S2), from values <4 x 10^3 s^{-2} in the east to ~5 x 10^3 s^{-2} in the west. Increasing stratification from east to west likely relates to warming of SST, and interactions with the Agulhas Current (Poulton et al., 2022).

SML NO_3 ranged from 0.1-6.2 µmol N L^{-1} (average: 1.1 (± 1.4) µmol N L^{-1}), with similar concentrations in the east and west (Table S2). Relative to PO_4, as indicated by N* values, NO_3 was always deficient (always negative) relative to Redfield (1958) (Table S2, Poulton et al., 2022). Strong negative values (-6 to -2.5) were related to the subtropical source waters for the AB (Poulton et al., 2022). SML $Si(OH)_4$ ranged from 0.6-5.1 µmol Si L^{-1} (average: 2.9 (± 1.1) µmol Si L^{-1}) (Table S2), higher than those found in the subtropical source water and highlighting the role of coastal upwelling in (re)supplying and retaining Si on the AB (Poulton et al., 2022). SML Si* values were mostly positive on the AB indicating residual silicic acid relative to NO_3 in autumn (Table S2).

3.2. Spatial Distribution of Phytoplankton Biomass

Satellite Chl concentrations ranged from <0.1-4.0 mg m-3 during autumn, with higher concentrations from east to west (Figure 1a). Surface in-situ Chl ranged from 0.3-4.7 mg m-3 (average: 2.1 (± 1.1) mg m-3) (Figure 1a). Around 46% of sampling stations had Chl >2 mg m-3 and no consistent spatial distribution was observed.

In terms of euphotic zone integrated biomass, PRO biomass ranged from 0.002-0.16 g C m^{-2} (average: 0.05 (± 0.04) g C m^{-2}) (Figure 1b). SYN biomass ranged from 0.002-0.05 g C m^{-2} (0.01 (±0.01) and was relatively high (>0.02 g C m^{-2}) at some of the inshore stations (e.g., transects 7, 9 and 12), while offshore stations exhibited lower (<0.01 g C m^{-2}) biomass (Figure 1c). Of all the groups, SYN biomass was the lowest. PICO biomass ranged from 0.006-0.13 g C m^{-2} (average: 0.04 (± 0.03) g C m^{-2}) (Figure 1d). NANO dominated biomass, with estimates ranging from 0.19-4.99 g C m^{-2} (average: 1.4 (± 1.2) g C m^{-2}) (Figure 1e). NANO biomass was much higher (>0.3 g C m^{-2}) than the other groups at ~100% of stations. CRYPTO biomass ranged from 0.002 to 1.09 g C m^{-2} (average: 0.12 (± 0.22) g C m^{-2}) (Figure 1f). No clear spatial patterns were observed for PRO, SYN, PICO, or NANO (Figures 1b-e), though there was a noticeable increase in CRYPTO biomass from east to west (Figure 1f).

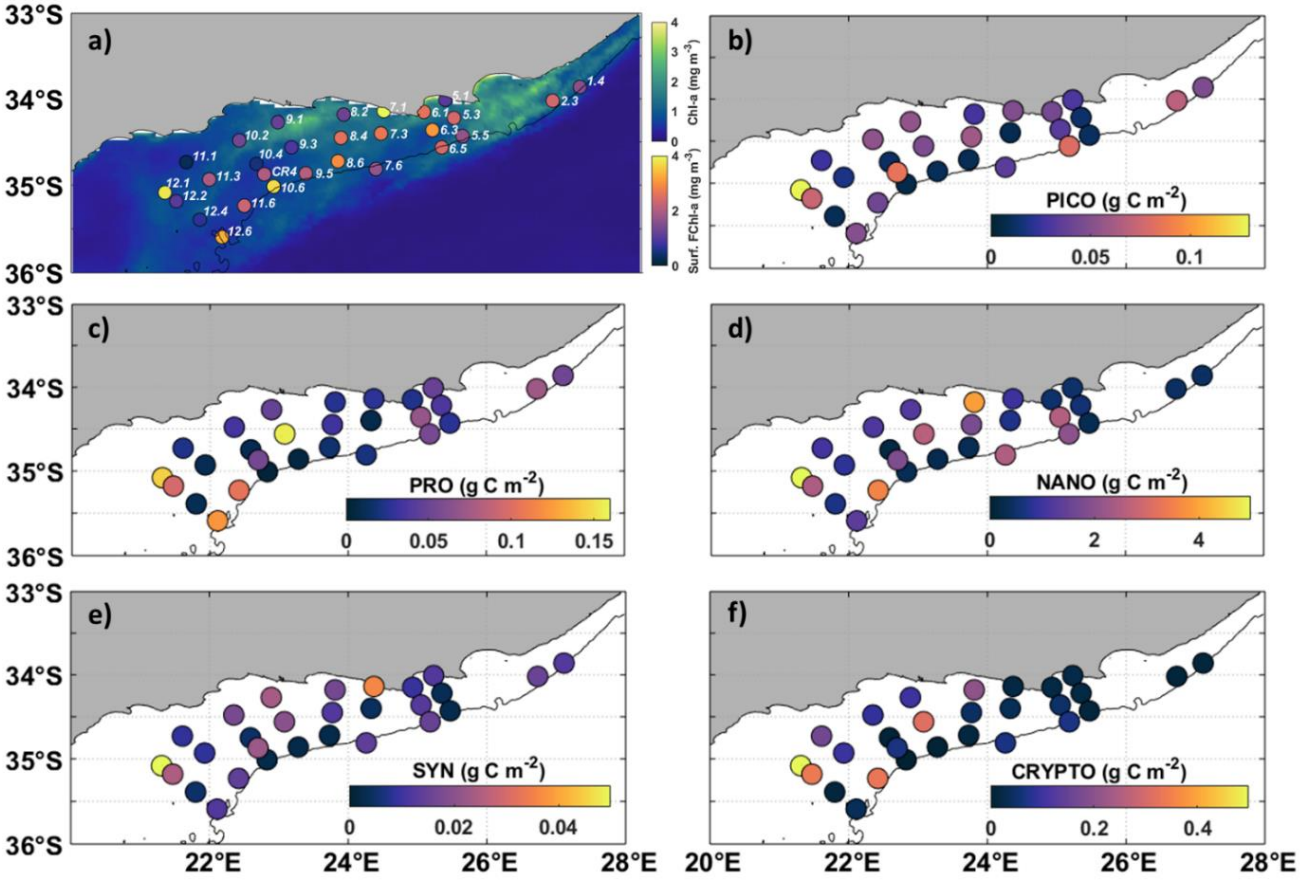

Figure 1. Phytoplankton biomass distribution on the Agulhas Bank in autumn. (a) Surface calibrated-fluorescence FChl (mg m^{-3}) superimposed on an 8-day composite (28/2/2019 – 06/3/2019) of satellite Chl (4 km Ocean Colour Climate Change Initiative (OCCI) data); euphotic zone integrated biomass (g C m^{-2}) of each group (b) PRO, (c) SYN, (d) PICO, (E) NANO, and (F) CRYPTO. Bathymetry marks the 200 m isobath.

3.3. Vertical Distribution of Phytoplankton Biomass

A sub-surface Chl maximum (SCM) occurred at ~50% of the stations sampled on the AB (Poulton et al., 2022), ranging in depth from 9 to 41 m and exhibiting no clear spatial pattern between stations. Generally, the vertical distribution of the different groups in terms of biomass was variable amongst the sampled stations. The depth of maximum biomass varied throughout the sampled stations and between the different groups. To examine the vertical distribution of small phytoplankton biomass, box-and-whisker plots of group biomass concentrations for surface waters, the SCM and at the base of the euphotic zone (Z_{eu}) are presented in Figure 2. None of the five groups examined (PRO, SYN, PICO, NANO, CRYPTO) showed any general depth preferences (Kruskal-Wallis t-tests, $p > 0.05$ for all groups and depth), though the median biomass for all groups was slightly higher in the SCM than surface or deeper waters

(Figures 2a-e). Overall, NANO exhibited higher biomass (>0.05 g C m^{-3}; Figure 2d) than all the other groups for the depths examined (Figures 2a-e).

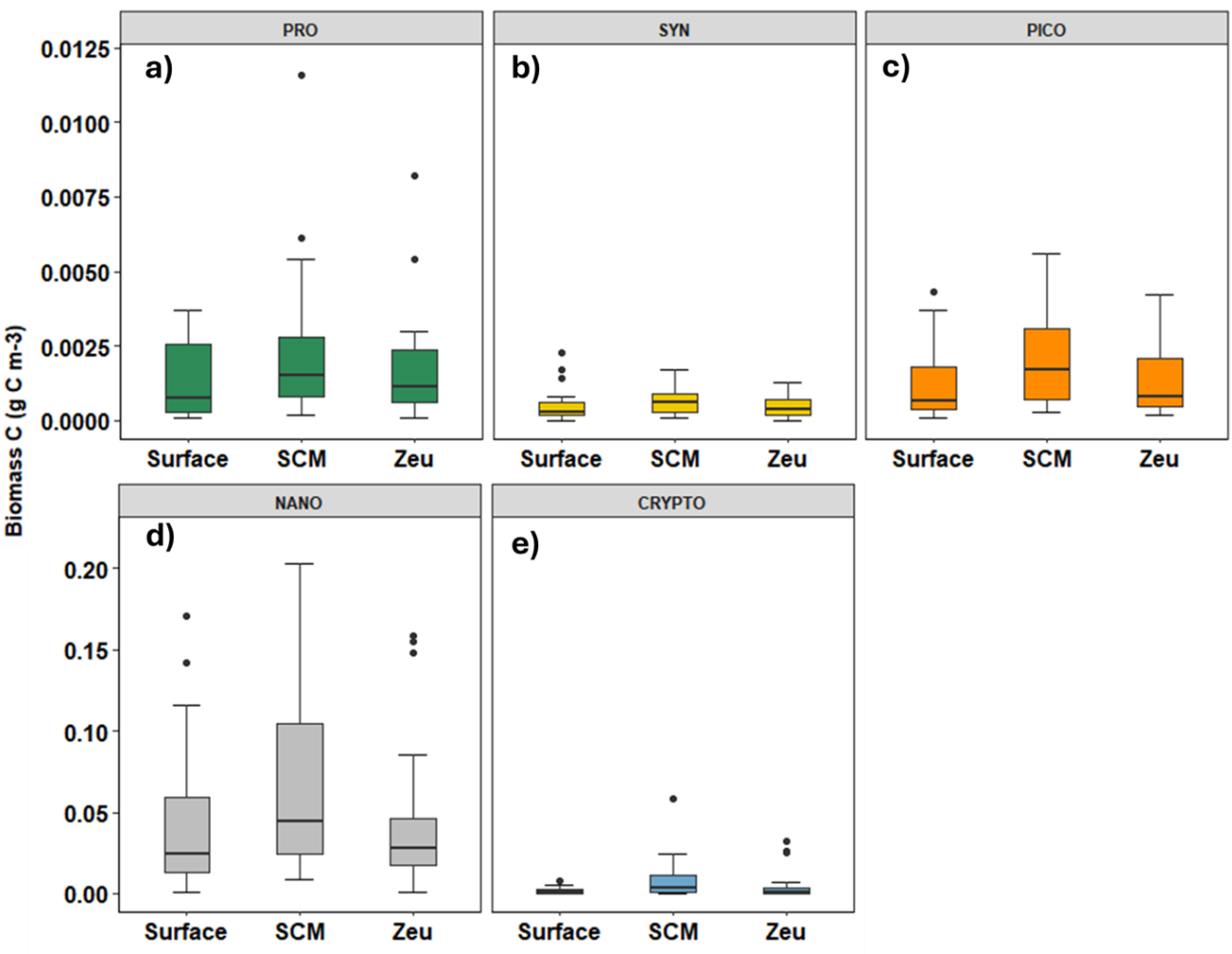

Figure 2. Boxplots of biomass (g C m^{-3}) in surface waters, the sub-surface chlorophyll maximum (SCM) and at the base of the euphotic depth (Zeu) for each group (a) PRO, (b) SYN, (c) PICO, (d) NANO, and (e) CRYPTO. The boxplots indicate values of median (solid horizontal line), 25^{th} and 75^{th} percentiles (box ranges), confident intervals (whiskers), and outliers (black dots).

3.4. Size-structure of the Phytoplankton Community

In surface waters, NANO dominated (average: 85 (± 9.9) %) community biomass (Figure 3a), with lower and more similar average contributions from PRO (5.1 (± 5.8) %), CRYPTO (4.4 (± 5.4) %) and PICO (4.0 (± 3.6) %), and much lower contributions from SYN (1.3 (± 0.9) %). NANO contributions to surface phytoplankton biomass were always >70%, while PRO

contributions were always <15% and only at 6 stations were the contributions >5% (Figure 3a). SYN contributions to surface phytoplankton biomass were always <3%, while PICO and CRYPTO were always less than 20% and 15%, respectively.

For euphotic zone integrated biomass (Figure 3b), NANO were again dominant (87 (± 5.7) %), with lower and more similar contributions from CRYPTO (4.9 (± 4.1) %), PRO (3.6 (± 2.8) %) and PICO (3.3 (± 2.4) %), and SYN contributions ~1% (1.1 (± 0.7) %). PRO biomass contribution decreased on average from east to west (5.0 to 2.8%) while CRYPTO contributions increased east to west (2.8 to 6.2%), whereas no clear trend was evident for the other groups. Low (<2%) contributions for SYN were a consistent feature in both surface waters (Figure 3a) and integrated biomass over the euphotic zone on the AB in autumn (Figure 3b).

Whether in carbon (Figures 3a & b) or Chl-a biomass (Figure 3c; Poulton et al., 2022), the nanoplankton (2-20 µm) were the dominant size class on the AB in autumn. On average, nanoplankton Chl (NANO+CRYTO) represented 63.1 (± 11.9) % of total Chl-a, while picoplankton Chl (PRO+SYN+PICO) represented 36.9 (± 11.9) % (Figure 3c). Picoplankton contributions to total Chl-a increased east to west (30.4 to 41.0%), while nanoplankton Chl decreased east to west (69.6 to 59.0%). Measurements of microplankton Chl (>20 µm; Poulton et al., 2022) showed low contributions (<30%) across most of the AB, with few stations characterised by microplankton dominance (not shown).

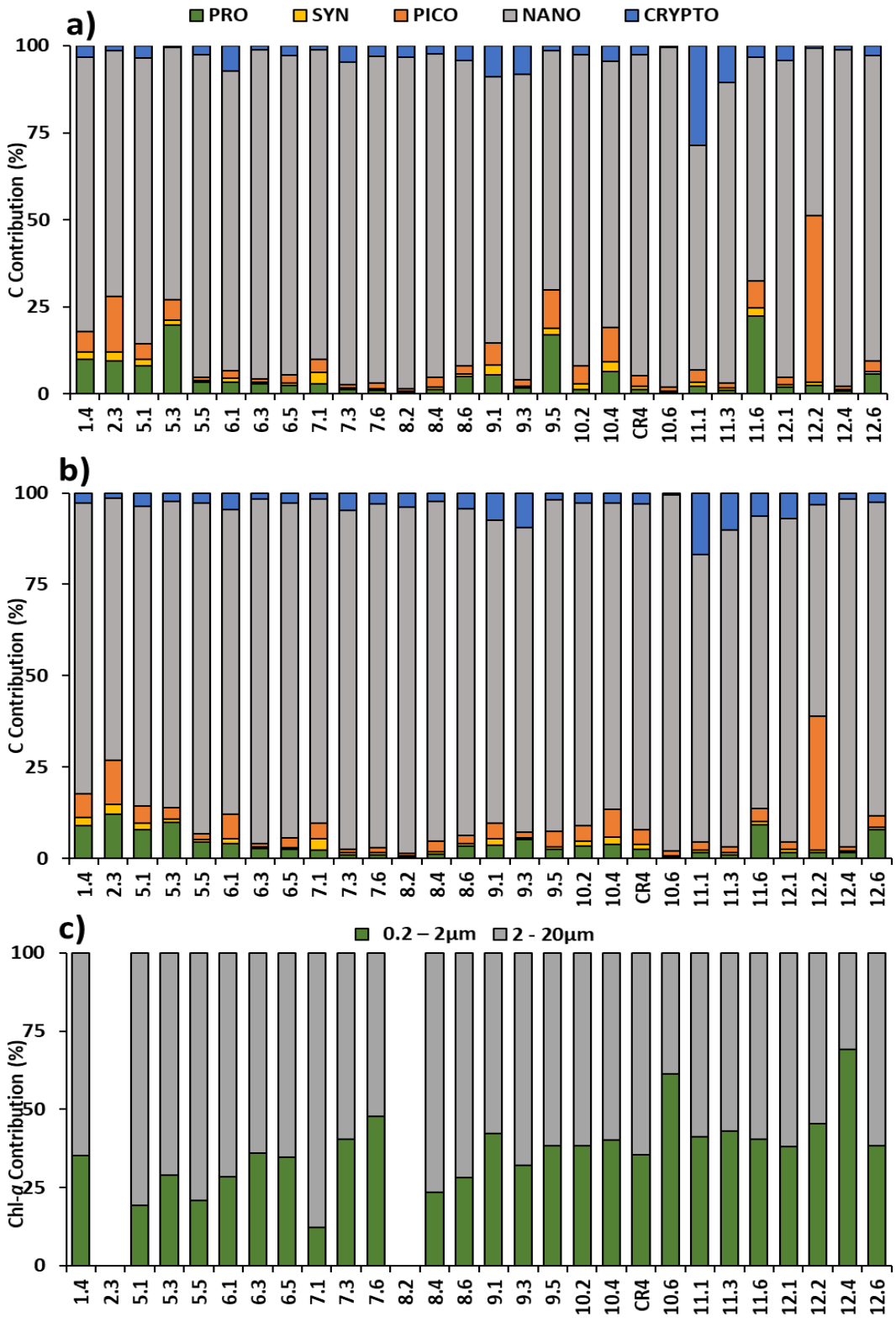

Figure 3. Phytoplankton group contributions (%) to total carbon biomass for surface waters (a) and integrated euphotic zone (b), and for integrated size fractionated Chl (c). PRO, SYN, PICO, NANO and CRYPTO. (c) size fractionated Chl (Poulton et al., 2022) for picoplankton (0.2-2 µm) and nanoplankton (2-20 µm) in the euphotic zone.

3.5. Phytoplankton Biomass and Agulhas Bank Hydrography

To explore the relationship between environmental conditions and phytoplankton composition, variability in hydrography (SST, $\bar{E}_{SML}$, N^2 max., and SML average nutrient concentrations [NO_3, $Si(OH)_4$]) was assessed with a Principal Component Analysis (PCA) (R vegan package). PC1 explained 44% of the variance between stations, while PC2 explained 27% and three next PCs explained less than 15% each. PC1 describes an inverse relationship between SST and nutrient (NO_3, $Si(OH)_4$) concentrations (Table 1); warmer waters were more nutrient poor on the AB. PC2 describes an inverse relationship between stratification (N^2 max.) and $\bar{E}_{SML}$ (Table 1); with stronger stratification leading to shallower SML and higher average irradiances.

Though PC1 and PC2 reflected the spatial variability in hydrographic conditions across the AB (see also Poulton et al., 2022), Pearson correlation showed that there was limited co-variability with phytoplankton biomass or community composition (Table 1). Only the absolute biomass of PICO and SYN showed (negative) statistically significant ($p<0.05$) correlations with PC1; no statistically significant correlations were observed with the biomass of the other groups present on the AB (Table 1). This highlights higher biomass of PICO and SYN warmer, more nutrient poor waters on the AB. No correlations were observed between either PCs and the percentage contribution of the different groups to total biomass (Table 1).

Table 1. Results of Principal Component Analysis (PCA), including eigenvalues and Pearson correlation coefficients for the relationships between PC scores, hydrographic variables, and absolute and relative phytoplankton group biomass (n = 28). *p < 0.05; **p < 0.01; ***p < 0.005.

Hydrography	**SST**	**$\bar{E}_{SML}$**	**N^2 max.**	**SML NO_3**	**SML $Si(OH)_4$**
PC-1	-1.4 (**-0.92*****)	0.44 (0.29)	-0.39 (-0.26)	1.30 (**0.85*****)	1.06 (**0.70*****)
PC-2	-0.28 (-0.19)	-1.04 (**-0.68*****)	1.14 (**0.75*****)	-0.26 (-0.17)	0.79 (0.52**)
	PRO	**SYN**	**PICO**	**NANO**	**CRYPTO**
Absolute Biomass					
PC-1	-0.36	-0.41*	-0.45*	-0.27	-0.28
PC-2	-0.09	0.2	-0.004	-0.06	0.06
Relative Biomass					
PC-1	-0.02	-0.10	-0.1	0.29	-0.32
PC-2	-0.26	0.17	-0.07	0.03	0.16

4. Discussion

The average integrated biomass for the pico- and nanoplankton on the AB in autumn was 1.6 g C m^{-2} (range:0.2 to 6.4 g C m^{-2}) which agrees well with a value of 1.9 g C m^{-2} for the global ocean (Buitenhuis et al., 2012) and ~2.2 g C m^{-2} for similar regional shelf sea studies (e.g., Agusti et al., 2019; Wei et al., 2020; Chen et al., 2021). Overall, NANO showed the highest contribution (average: 87%; range: 73 to 96%) to the total carbon biomass in surface, SCM and integrated over the water column, with all other groups contributing less than 5%. Dominance of phytoplankton biomass by nanoplankton agrees well with the size fractionated pigment data from Poulton et al. (2022), highlighting higher contributions to total Chl of nanoplankton than either pico- or microplankton.

On the east coast of South Africa, Barlow et al. (2002, 2020) reported elevated biomass and a co-dominance between diatoms and haptophytes on the far eastern stations between 26.5 and 27.5 °E due to the upwelling of nutrient rich waters. This is indicative of the nanoplankton dominance in the region upstream (east) of our sampling area. Lamont et al. (2018) also highlighted nanoplankton as important to the AB despite showing a lower contribution than microplankton. The nano-sized group has been observed to be more prominent in warmer shelf waters, where they are able to take advantage of high nutrient concentrations (Barlow et al., 2001, 2017).

Despite the highly stratified nature of the AB (Carter et al., 1987; Largier and Swart, 1987), the distribution of pico- and nanoplankton biomass for the different groups showed no strong vertical patterns (Figure 2). Though biomass of all groups was slightly higher in the SCM, these differences were not statistically significant and the SCM did not represent a strong biomass maximum as found in other shelf sea systems (e.g., Mena et al., 2019; Barnett et al., 2019). During autumn on the AB, light availability in the SCM decreased from east to west (Poulton et al., 2022), this is likely linked to peak biomass observed on some stations on the west, and thus may have prevented strong biomass maxima forming at depth. Previous studies on the central AB have observed SCM with considerable Chl concentrations (>10 mg m^{-3}) and phytoplankton biomass (Carter et al., 1987), though such high Chl SCM were not observed during autumn in 2019.

While the AB had identifiable gradients in hydrographic conditions, as recognised in the PCA (Table 1) and other related studies (Poulton et al., 2022; Noyon et al., 2022), there were few

clear relationships between phytoplankton group biomass or community composition. Only PRO and SYN biomass correlated with PC1, indicating that these groups had higher biomass in warmer, more nutrient impoverished waters, potentially linked to the offshore Agulhas Current (Probyn et al., 1994; Jackson et al., 2012; Malan et al., 2018). This lack of linkage between phytoplankton biomass and composition potentially relates to non-limiting nutrient and light conditions (Poulton et al., 2022) across the section of the bank sampled in autumn 2019 (i.e., not near coast or off shelf waters).

Alternatively, nanoplankton dominance on the AB in autumn may be linked to the importance of grazing in controlling community composition. Indeed, a strong link between NPP and secondary production was observed in autumn 2019 (Noyon et al., 2022; Poulton et al., 2022), and an importance of microzooplankton as active grazers and agents of trophic transfer on the bank has been highlighted before (Huggett et al., 2023). Globally, ~64% of phytoplankton daily primary production is grazed by micro-zooplankton, with the smaller pico- and nanoplankton readily grazed by planktonic ciliates, heterotrophic flagellates, and small zooplankton (Calbet and Landry, 2004; Mayers et al., 2019).

With the warming of the ocean, it is expected that the phytoplankton will shift from large-species dominance to smaller nano-sized phytoplankton (Bopp et al., 2005; Lomas et al., 2012; Dutkiewicz et al., 2013; Henson et al., 2021). This will in turn have a large impact on the grazers, suggesting a decrease in food quality and a shift in the size structure of zooplankton from large to smaller groups (Safi et al., 2023). Our study further highlights the importance of microzooplankton on the AB in autumn, warranting further attention on these organisms in supporting the ecosystems of the AB.

A shift in the global trends of phytoplankton size structure from large to smaller sized phytoplankton has previously been observed and is projected in the future (Bopp et al., 2005; Lomas et al., 2012; Dutkiewicz et al., 2013; Henson et al., 2021). This is mainly attributed to the warming of the oceans and a depletion of nutrient supplies, giving advantage to the nano- and picoplankton communities to flourish. The dominance of nanoplankton biomass on the AB shelf ecosystem is comparable to other shelf regions. A similar shift in the community from the larger phytoplankton to the smaller phytoplankton was also indicated by Huggett et al. (2023). On the AB, where there has been a scarcity of in-situ sampling of the plankton community, shifts in size structure may have severe implications for the ecosystems supported by AB productivity and there is an urgent need for further studies.

Author contributions

Conceptualization: Sixolile L. Mazwane, Alex J. Poulton, Margaux Noyon. **Formal analysis:** Sixolile L. Mazwane, Alex J. Poulton, Margaux Noyon, Emma Rocke. **Investigation:** Sixolile L. Mazwane, Alex J. Poulton. **Methodology:** Sixolile L. Mazwane, Alex J. Poulton, Margaux Noyon, Emma Rocke. **Writing – original draft:** Sixolile L. Mazwane, Alex J. Poulton, Margaux Noyon. **Writing – review & editing:** Sixolile L. Mazwane, Alex J. Poulton, Margaux Noyon, Emma Rocke. **Project administration and Funding Acquisition:** Mike J. Roberts.

Conflict of interest

The authors declare no conflicts of interest relevant to this study.

Data Availability Statement

Chlorophyll, CTD and nutrient data from EK188 is available through the British Oceanographic Data Centre (BODC) at doi:10.5285/d5cea266-fbec-7ef0-e053-6c86abc0722c. Flow cytometry count data has been submitted to Zenodo and can be accessed at https://doi.org/10.5281/zenodo.10674482.

Acknowledgements

We thank the captain and crew of the R/V *Ellen Khuzwayo*, together with the Department of Forestry, Fisheries, and the Environment (DFFE). This study was produced with the financial support of the Global Challenges Research Fund (GCRF), UK, in the framework of the SOLSTICE-WIO project, under NERC grant NE/P021050/1. This work was also part of the UK-SA bilateral chair Ocean Science and marine food security funded by the NRF/DST Grant (98399) and the British Council grant SARCI150326116102. We thank the Health Sciences department at the University of Cape Town (UCT) for the use of their Flow Cytometer. We would like to thank the ESA Ocean Colour CCI project for processing and providing the *Chl-a* dataset online at http://www.esa-o ceancolour-cci.org/.

References

Acevedo-Trejos, E., Brandt, G., Bruggeman, J., & Merico, A. (2015). Mechanisms shaping size structure and functional diversity of phytoplankton communities in the ocean. Scientific Reports, 5, 17–20. https://doi.org/10.1038/srep08918

Agusti, S., Lubián, L.M., Moreno-Ostos, E., Estrada, M., & Duarte, C.M., 2019. Projected Changes in Photosynthetic Picoplankton in a Warmer Subtropical Ocean. Front. Mar. Sci. 5:506. doi: 10.3389/fmars.2018.00506

Barlow, R. G., Lamont, T., Kyewalyanga, M., Sessions, H., Morris, T., Carter, R. A., et al. (2001). Chapter 6 : Latitudinal Changes in the Shape, Formation and Ecology of the Chlorophyll a Maximum in the Subtropical and. South African Journal of Marine Science, 54(1), 525–536. https://doi.org/10.1016/j.rse.2017.09.038

Barlow, R. G., Aiken, J., Holligan, P. M Oceanographic Research Papers, 49(4), 637–660. https://doi.org/10.1016/S0967-0637(01)00081-4

Barlow, R., Lamont, T., Kyewalyanga, M., Sessions, H.,., Cummings, D. G., Maritorena, S., & Hooker, S. (2002). Phytoplankton pigment and absorption characteristics along meridional transects in the Atlantic Ocean. Deep-Sea Research Part I: & Morris, T. (2010). Phytoplankton production and physiological adaptation 30(13), 1472–1486. https://doi.org/10.1016/j.csr.2010.05.007

Barlow, R., Lamont, T., Gibberd, M. J., Airs, R., Jacobs, L., & Britz, K. (2017). Phytoplankton communities and acclimation in a cyclonic eddy in the southwest Indian Ocean. Deep-Sea Research Part I: Oceanographic Research Papers, 124, 18–30. https://doi.org/10.1016/j.dsr.2017.03.013

Barlow, R., Lamont, T., Gibberd, M. J., Russo, C., Airs, R., Tutt, G., et al. (2020). Phytoplankton adaptation and absorption properties in an Agulhas Current ecosystem. Deep-Sea Research Part I: Oceanographic Research Papers, 157(December 2019), 103209. https://doi.org/10.1016/j.dsr.2019.103209

Barnett, M.L., Kemp, A.E.S., Hickman, A.E. & Purdie, D.A. (2019). Shelf Sea subsurface chlorophyll maximum thin layers have a distinct phytoplankton community structure. Continental Shelf Research, Volume 174, 2019, 140-157, https://doi.org/10.1016/j.csr.2018.12.007.

Becker, S., Aoyama, M., Woodward, E.M.S., Bakker, K., Coverly, S., Mahaffey, C., & Tanhua, T.(2020). GO-SHIP repeat hydrography nutrient manual: the precise and accurate determination of dissolved inorganic nutrients in seawater, using continuous flow analysis methods. Front. Mar. Sci. 7, 581790. https://doi.org/10.3389/fmars.2020.581790.

Bibby, T. S., & Moore, C. M. (2011). Silicate:nitrate ratios of upwelled waters control the phytoplankton community sustained by mesoscale eddies in sub-tropical North Atlantic and Pacific. Biogeosciences, 8(3), 657–666. https://doi.org/10.5194/bg-8-657-2011

Bopp, L., Aumont, O., Cadule, P., Alvain, S., & Gehlen, M. (2005). Response of diatoms distribution to global warming and potential implications: A global model study, Geophys. Res. Lett., 32, L19606, doi:10.1029/2005GL023653, 2005

Børsheim, K.Y., Bratbak, G. (1987). Cell volume to cell carbon conversion factors for a bacterivorous Monas sp. enriched from seawater. Mar. Ecol. Prog. Ser. 36, 171–175.

Brzezinski, M.A. (1985). The Si:C:N ratio of marine diatoms: interspecific variability and the effect of some environmental variables. J. Phycol. 21, 347–357. https://doi.org/10.1111/j.0022-3646.198.00347.x.

Buitenhuis, E.T., Li, W.K.W., Vaulot, D., Lomas, M.W., Landry, M.R., Partensky, F., Karl, D.M., Ulloa, O., Campbell, L., Jacquet, S., Lantoine, F., Chavez, F., MacIas, D., Gosselin, M., McManus, G.B. (2012). Picophytoplankton biomass distribution in the global ocean. Earth Syst. Sci. Data 4, 37–46. https://doi.org/10.5194/essd-4-37-2012

Calbet, A., & Landry, M. R. (2004). Phytoplankton growth, microzooplankton grazing, and carbon cycling in marine systems. Limnology and Oceanography, 49(1), 51–57. https://doi.org/10.4319/lo.2004.49.1.0051

Campbell, L. (2001). Flow Cytometric Analysis of Autotrophic Picoplankton, Methods in Microbiology. Academic Press, pp. 317–343.

Carter, R. A., Mcmurray, H. F., Largier, J. L., McMurray, H. F., & Thermocline, J. L. L. (1987). Thermocline characteristics and phytoplankton dynamics in Agulhas Bank waters. South African Journal of Marine Science, 5(1), 327–336. https://doi.org/10.2989/025776187784522306.

Carvalho, F., Kohut, J., Oliver, M.J. & Schofield, O. (2017). Defining the ecologicallyrelevant mixed-layer depth for Antarctica's coastal seas. Geophys. Res. Lett. 44, 338–345. https://doi.org/10.1002/2016GL071205.

Chen, T.Y., Lai, C.C., Tai, J.H., Ko, C.Y., Shiah, F.K. (2021). Diel to Seasonal Variation of Picoplankton in the Tropical South China Sea. Front. Mar. Sci. 8, 1–12. https://doi.org/10.3389/fmars.2021.732017.

Chisholm, S. W., Olson, R. J., Zettler, E. R., Goericke, R., Waterbury, J. B. & Welschmeyer, N. A. (1988). A novel free-living prochlorophyte abundant in the oceanic euphotic zone. Nature, 334, 340–343.

Daneri, G., Lizárraga, L., Montero, P., González, H.E., Tapia, F.J. (2012). Wind forcing and short-term variability of phytoplankton and heterotrophic bacterioplankton in the coastal zone of the Concepcion upwelling system (Central Chile). Prog. Ocea., 92-96.

Dutkiewicz, S., Scott, J. R. & Follows, M. J. (2013). Winners and losers: ecological and biogeochemical changes in a warming ocean. Glob. Biogeochem. Cycles 27, 463-477.

Field, C. B., Behrenfeld, M. J., Randerson, J. T., & Falkowski, P. (1998). Primary production of the biosphere: Integrating terrestrial and oceanic components. Science, 281(5374), 237–240. https://doi.org/10.1126/science.281.5374.237

Flander-Putrle, V., Francé, J., & Mozetič, P. (2021). Phytoplankton pigments reveal size structure and interannual variability of the coastal phytoplankton community (Adriatic Sea). Water (Switzerland), 14(1). https://doi.org/10.3390/w14010023

Flombaum, P., Wang, WL., Primeau, F.W. et al. (2020). Global picophytoplankton niche partitioning predicts overall positive response to ocean warming. Nat. Geosci. 13, 116–120. https://doi.org/10.1038/s41561-019-0524-2

Henson, S.A., Cael, B.B., Allen, S.R. & Dutkiewicz, S. (2021). Future phytoplankton diversity in a changing climate. Nat Commun 12, 5372. https://doi.org/10.1038/s41467-021-25699-w

Huggett, J. A., Noyon, M., Carstensen, J., & Walker, D. R. (2023). Patterns in the plankton – Spatial distribution and long-term variability of copepods on the Agulhas Bank. Deep-Sea Research Part II: Topical Studies in Oceanography, 208, 105265. https://doi.org/10.1016/j.dsr2.2023.105265

Hutchings, L., van der Lingen, C.D., Shannon, L.J., Crawford, R.J.M., Verheye, H.M.S., Bartholomae, C.H., van der Plas, A.K., Louw, D., Kreiner, A., Ostrowski, M., Fidel,

Q., Barlow, R.G., Lamont, T., Coetzee, J., Shillington, F., Veitch, J., Currie, J.C., & Monteiro, P.M.S. (2009). The Benguela Current: an ecosystem of four components. Prog. Oceanogr. 83, 15–32. http://dx.doi.org/10.1016/j.pocean.2009.07.046.

Hydes, D. J., Aoyama, M., Aminot, A., Bakker, K., Becker, S., Coverly, S., et al. (2010). Determination of dissolved nutrients (N, P, Si) in seawater with high precision and inter- comparability using gas-segmented continuous flow analysers, In: The GO-SHIP repeat hydrography manual: A collection of expert reports and guidelines. IOCCP report No. 14. ICPO publication series No. 134.

Jackson, J. M., Rainville, L., Roberts, M. J., McQuaid, C. D., & Lutjeharms, J. R. E. (2012). Mesoscale bio-physical interactions between the Agulhas Current and the Agulhas Bank, South Africa. Continental Shelf Research, 49, 10–24. https://doi.org/10.1016/j.csr.2012.09.005

Lamont, T., Brewin, R. J. W., & Barlow, R. G. (2018). Seasonal variation in remotely-sensed phytoplankton size structure around southern Africa. Remote Sensing of Environment, 204, 617–631. https://doi.org/10.1016/j.rse.2017.09.038

Liang, Y., Zhang, Y., Zhang, Y., Luo, T., Rivkin, R. B. and Jiao, N. (2017). Distributions and relationships of virio- and picoplankton in the epi-, meso- and bathypelagic zones of the Western Pacific Ocean. FEMS Microbiology Ecology 93(2), fiw238

Liu, H., Probert, I., Uitz, J., Claustre, H., Aris-Brosou, S., Frada, M., et al. (2009). Extreme diversity in noncalcifying haptophytes explains a major pigment paradox in open oceans. Proceedings of the National Academy of Sciences of the United States of America, 106(31), 12803–12808. https://doi.org/10.1073/pnas.0905841106

Lomas, M. W., Moran, S. B., Casey, J. R., Bell, D. W., Tiahlo, M., Whitefield, J., et al. (2012). Spatial and seasonal variability of primary production on the Eastern Bering Sea shelf. Deep-Sea Research Part II: Topical Studies in Oceanography, 65–70, 126–140. https://doi.org/10.1016/j.dsr2.2012.02.010

Malan, N., Backeberg, B., Biastoch, A., Durgadoo, J. V., Samuelsen, A., Reason, C., & Hermes, J. (2018). Agulhas Current meanders facilitate shelf-slope exchange on the Eastern Agulhas Bank. Journal Geophysical Research: Oceans, 123, 4762–4778. https://doi.org/10.1029/2017JC013602

Marañón, E. (2015). Cell size as a key determinant of phytoplankton metabolism and community structure. Ann Rev Mar Sci. 7:241-64. doi: 10.1146/annurev-marine-010814- 015955. Epub 2014 Jul 25. PMID: 25062405.

Marie, D., Partensky, F., Jacquet, S., Vaulot, D. (1997). Enumeration and cell cycle analysis of natural populations of marine picoplankton by flow cytometry using the nucleic acid stain SYBR Green I. Appl. Environ. Microbiol. 63, 186–193.

Mayers, K. M. J., Poulton, A. J., Daniels, C. J., Wells, S. R., Woodward, E. M. S., Tarran, G. A., et al. (2019). Growth and mortality of coccolithophores during spring in a temperate Shelf Sea (Celtic Sea, April 2015). Progress in Oceanography, 177, 101928. https://doi.org/10.1016/j.pocean.2018.02.024

Mazwane, S. L., Poulton, A. J., Hickman, A. E., Jebri, F., Jacobs, Z., Roberts, M., & Noyon, M. (2022). Spatial and temporal variability of Net Primary Production on the Agulhas Bank, 1998–2018. Deep-Sea Research Part II: Topical Studies in Oceanography, 199, 105079. https://doi.org/10.1016/j.dsr2.2022.105079

Mena, C., Reglero, P., Hidalgo, M., Sintes, E., Santiago, R., Martín, M., Moyà, G. & Balbín, R. (2019). Phytoplankton Community Structure Is Driven by Stratification in the Oligotrophic Mediterranean Sea. Front. Microbiol. 10:1698. doi:10.3389/fmicb.2019.01698

Mitra, A., Caron, D.A., Faure, E., Flynn, K.J., Gonçalves Leles, S., Hansen, P.J. et al. (2023). The Mixoplankton database (MDB). Zenodo. https://doi.org/10.5281/zenodo.7560583

Moore, C. M., Suggett, D., Holligan, P. M., Sharples, J., Abraham, E. R., Lucas, M. I., et al. (2003). Physical controls on phytoplankton physiology and production at a shelf sea front: A fast repetition-rate fluorometer based field study. Marine Ecology Progress Series, 259, 29–45. https://doi.org/10.3354/meps259029

Moore, C.M., Mills, M.M., Achterberg, E.P., Geider, R.J., LaRoche, J., Lucas, M.I., McDonagh, E.L., Pan, X., Poulton, A.J., Rijkenberg, M.J.A., Suggett, D.J., Ussher, S. J. & Woodward, E.M.S. (2009). Large-scale distribution of Atlantic nitrogen fixation controlled by iron availability. Nat. Geosci. 2, 867–871. https://doi.org/10.1038/ngeo667.

Moran, M. A., 2015. The global ocean microbiome. Science.350(6225), aac8455.

Noyon, M. (2019). Oceanographic Survey of the Eastern and Central Agulhas Bank (South Africa). Port Elizabeth.

Noyon, M., Poulton, A.J., Asdar, S., Weitz, R., Giering, S.L.C. (2022). Mesozooplankton community distribution on the Agulhas Bank in autumn: Size structure and production. Deep. Res. Part II Top. Stud. Oceanogr. 195, 105015. https://doi.org/10.1016/j.dsr2.2021.105015

Pauly, D., Christensen, V., Guénette, S., Pitcher, T. J., Sumaila, U. R., Walters, C. J., et al. (2002). Towards sustainability in world fisheries. Nature, 418 (6898), 689–695. https://doi.org/10.1038/nature01017

Poulton, A. J., Mazwane, S. L., Godfrey, B., Carvalho, F., Mawji, E., Wihsgott, J. U., & Noyon, M. (2022). Primary production dynamics on the Agulhas Bank in autumn. Deep-Sea Research Part II: Topical Studies in Oceanography, 203. https://doi.org/10.1016/j.dsr2.2022.105153

Poulton, A. J., Young, J. R., Bates, N. R., & Balch, W. M. (2011). Biometry of detached Emiliania huxleyi coccoliths along the Patagonian Shelf. Marine Ecology Progress Series, 443, 1–17. https://doi.org/10.3354/meps09445

Probyn, T. A., Mitchell-Innes, B. A., Brown, P. C., Hutchings, L., & Carter, R. A. (1994). A review of primary production and related processes on the Agulhas Bank. South African Journal of Science, 90, 166–173.

Rajaneesh, K. M., Mitbavkar, S., Anil, A. C., & Sawant, S. S. (2015). Synechococcus as an indicator of trophic status in the Cochin backwaters, west coast of India. Ecological Indicators, 55, 118-130.

Rajaneesh, K. M., Mitbavkar, S., & Anil, A. C. (2017). Influence of short-term hydrographic variations during the north-east monsoon on picophytoplankton community structure in the eastern Arabian Sea. Continental Shelf Research, 146, 28–36. https://doi.org/10.1016/j.csr.2017.08.008

Redfield, A.C. (1958). The biological control of chemical factors in the environment. Am. Sci. 46, 205–221. https://www.jstor.org/stable/27827150.

Safi, K. A., Rodríguez, A. G., Hall, J. A., & Pinkerton, M. H. (2023). Phytoplankton dynamics, growth and microzooplankton grazing across the subtropical frontal zone,

east of New Zealand. Deep-Sea Research Part II: Topical Studies in Oceanography, 208(January). https://doi.org/10.1016/j.dsr2.2023.105271

Scanlan D.J., Ostrowski, M., Mazard, S., Dufresne, A., Garczarek, L., Hess, W.R., Post, A.F., Hagemann, M., Paulsen, I., Partensky F. (2009). Ecological genomics of marine picocyanobacteria; Microbiology and molecular biology reviews 73(2), 249-299

Sieburth, J. (1979). Sea microbes. Oxford University Press New York

Sonnekus, M.J. (2020). Phytoplankton of the Southern Agulhas Large Marine Ecosystem (sACLME). PhD Thesis, Nelson Mandela University, Gqeberha (formerly Port Elizabeth), South Africa. Pp1-262

Tarran, G. A., Heywood, J. L., & Zubkov, M. V. (2006). Latitudinal changes in the standing stocks of nano- and picoeukaryotic phytoplankton in the Atlantic Ocean. Deep-Sea Research Part II: Topical Studies in Oceanography, 53(14–16), 1516–1529. https://doi.org/10.1016/j.dsr2.2006.05.004

Van Dongen-Vogels, V., Seymour, J.R., Middleton, J.F., Mitchell, J.G., Seuront, L. (2012). Shifts in picophytoplankton community structure influenced by changing upwelling conditions. Estuar. Coast. Shelf Sci. 109, 81–90. https://doi.org/10.1016/j.ecss.2012.05.026

Van Dongen-Vogels, V., Seymour, J.R., Middleton, J.F., Mitchell, J.G., Seuront, L. (2011). Influence of local physical events on picophytoplankton spatial and temporal dynamics in South Australian continental shelf waters. J. Plankton Res. 33, 1825–1841. https://doi.org/10.1093/plankt/fbr077

Wang, F., Wei, Y., Zhang, G., Zhang, L., & Sun, J. (2022). Picophytoplankton in the West Pacific Ocean: A Snapshot. Frontiers in Microbiology, 13, 1–13. https://doi.org/10.3389/fmicb.2022.811227

Waterbury, J. B., Watson, S. W., Guillard, R. R. L. et al. (1979) Widespread occurrence of a unicellular, marine planktonic, cyano- bacterium. Nature, 277, 293–294.Wei, Y., Huang, D., Zhang, G., Zhao, Y. & Sun, J. (2020). Biogeographic variations of picophytoplankton in three contrasting seas: The Bay of Bengal, South China Sea and western Pacific Ocean. Aquat. Microb. Ecol. 84, 91–103. https://doi.org/10.3354/ame01928

592 Wei, Y., Huang, D., Zhang, G., Zhao, Y., & Sun, J. (2020). Biogeographic variations of
593 picophytoplankton in three contrasting seas: The Bay of Bengal, South China Sea and
594 western Pacific Ocean. Aquatic Microbial Ecology, 84(1), 91–
595 103. https://doi.org/10.3354/ame01928

596 Worden, A. Z. (2006). Picoeukaryote diversity in coastal waters of the Pacific Ocean.
597 Aquatic Microbial Ecology, 43(2), 165-175.

Table 1. Results of Principal Component Analysis (PCA), including eigenvalues and Pearson correlation coefficients for the relationships between PC scores, hydrographic variables, and absolute and relative phytoplankton group biomass (n = 28). *p < 0.05; **p < 0.01; ***p < 0.005.

Hydrography	**SST**	**$\bar{E}_{SML}$**	**N^2 max.**	**SML NO_3**	**SML $Si(OH)_4$**
PC-1	-1.4 (**-0.92*****)	0.44 (0.29)	-0.39 (-0.26)	1.30 (**0.85***)	1.06 (**0.70***)
PC-2	-0.28 (-0.19)	-1.04 (**-0.68***)	1.14 (**0.75***)	-0.26 (-0.17)	0.79 (0.52**)
	PRO	SYN	PICO	NANO	CRYPTO
Absolute Biomass					
PC-1	-0.36	-0.41*	-0.45*	-0.27	-0.28
PC-2	-0.09	0.2	-0.004	-0.06	0.06
Relative Biomass					
PC-1	-0.02	-0.10	-0.1	0.29	-0.32
PC-2	-0.26	0.17	-0.07	0.03	0.16

Figure1.

Figure 1. Phytoplankton biomass distribution on the Agulhas Bank in autumn. (a) Surface calibrated-fluorescence FChl (mg m^{-3}) superimposed on an 8-day composite (28/2/2019 – 06/3/2019) of satellite Chl (4 km Ocean Colour Climate Change Initiative (OCCI) data); euphotic zone integrated biomass (g C m^{-2}) of each group (b) PRO, (c) SYN, (d) PICO, (E) NANO, and (F) CRYPTO. Bathymetry marks the 200 m isobath.

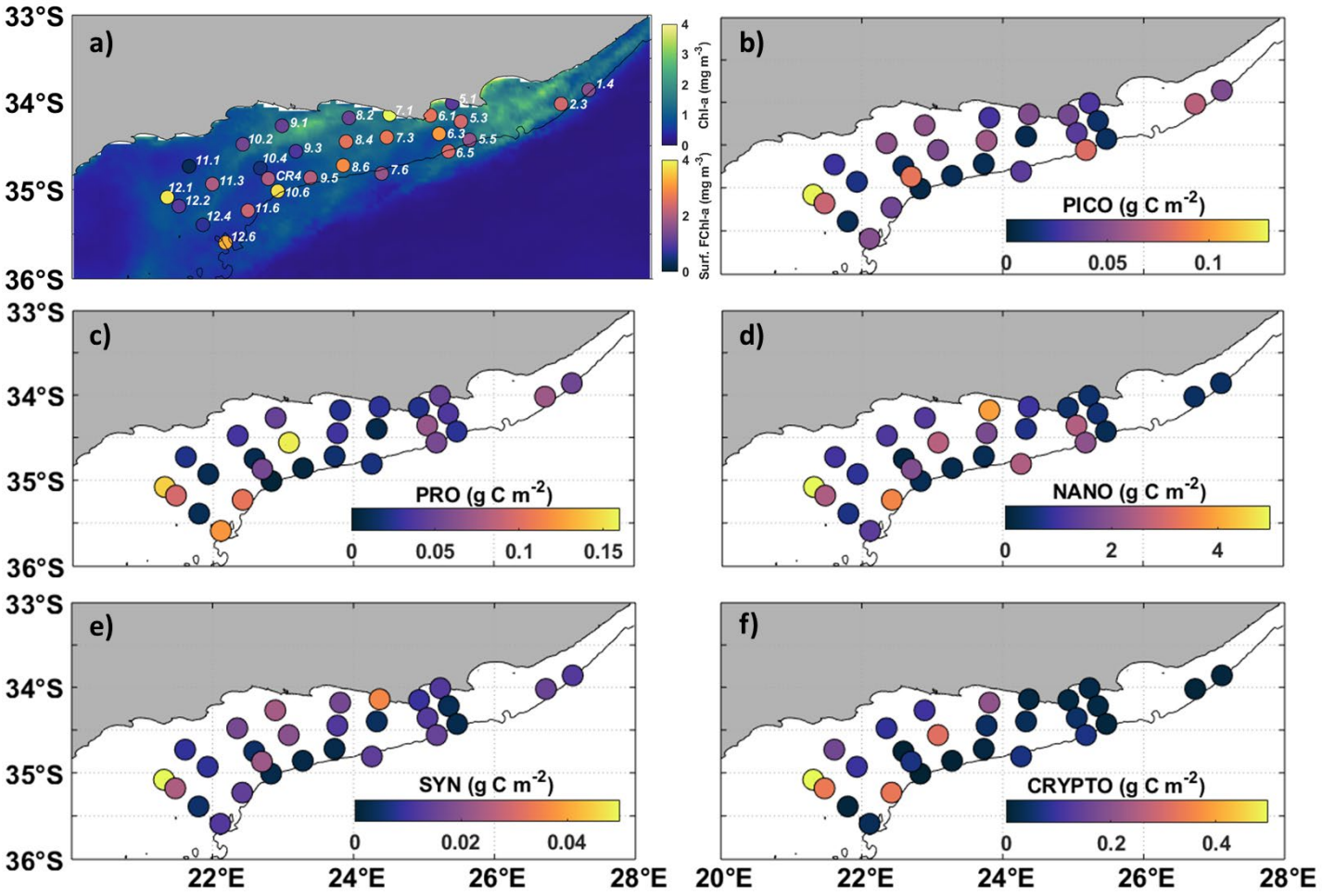

Figure2.

Figure 2. Boxplots of biomass (g C m^{-3}) in surface waters, the sub-surface chlorophyll maximum (SCM) and at the base of the euphotic depth (Z_{eu}) for each group (a) PRO, (b) SYN, (c) PICO, (d) NANO, and (e)CRYPTO. The boxplots indicate values of median (solid horizontal line), 25th and 75th percentiles (box ranges), confident intervals (whiskers), and outliers (black dots).

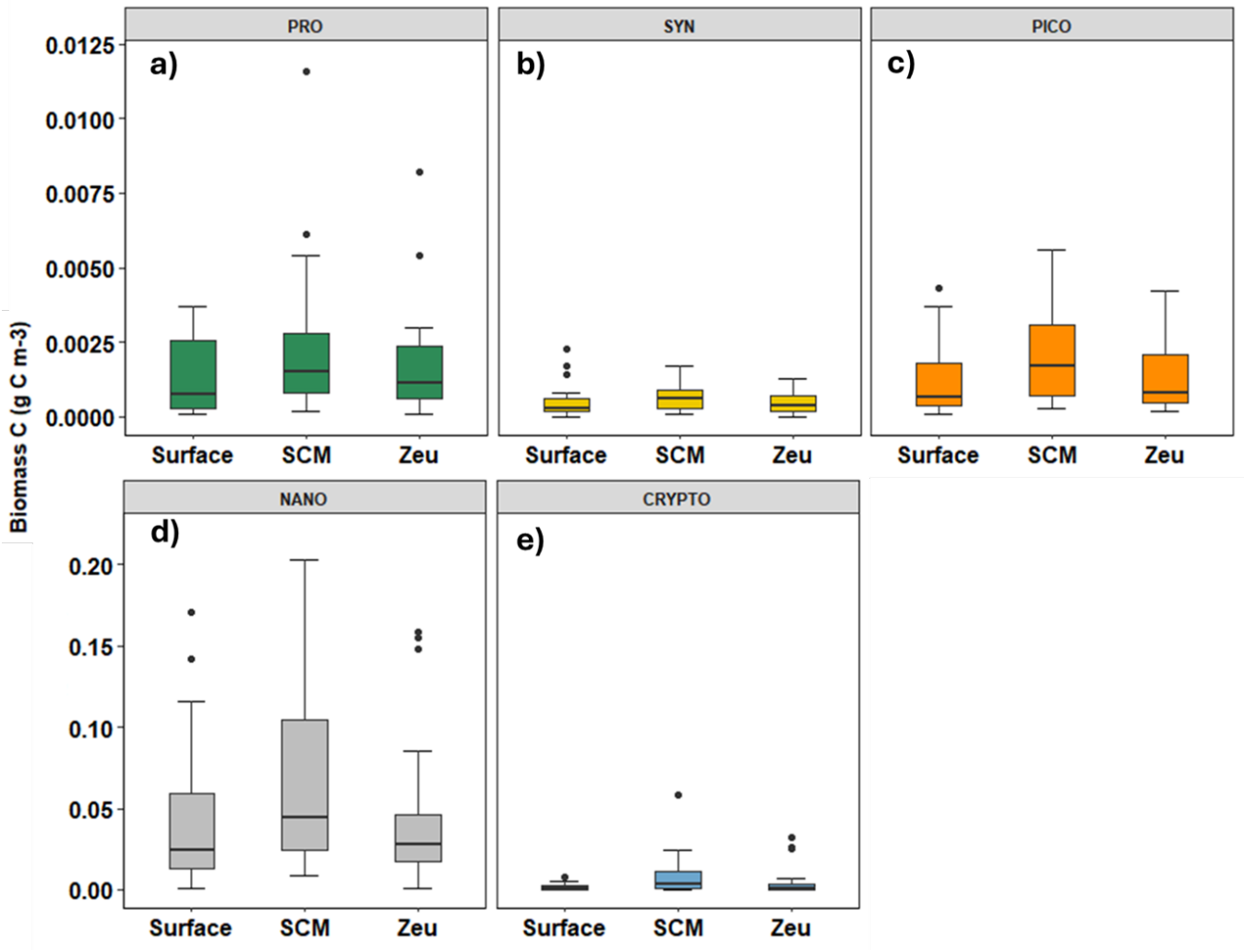

Figure3.

Figure 3. Phytoplankton group contributions (%) to total carbon biomass for surface waters (a) and integrated euphotic zone (b), and for integrated size fractionated Chl (c). PRO, SYN, PICO, NANO and CRYPTO. (c) size fractionated Chl (Poulton et al., 2022) for picoplankton (0.2-2 µm) and nanoplankton (2-20 µm) in the euphotic zone.